

On-Chip Silicon Photonic Thermometers: from Waveguide Bragg Grating to Ring Resonators sensors

Nikolai N. Klimov^{1,3}, Thomas Purdy², Zeeshan Ahmed²

¹*Thermodynamic Metrology Group, Sensor Science Division, Physical Measurement Laboratory, National Institute of Standards and Technology, Gaithersburg, MD, USA*

²*Quantum Optics Group, Quantum Measurement Division, Physical Measurement Laboratory, National Institute of Standards and Technology, Gaithersburg, MD, USA*

³*Joint Quantum Institute, University of Maryland, College Park, MD, USA*

Abstract

Fundamental limitations of resistance thermometry, as well as the desire to reduce sensor ownership cost has led to considerable interest in the development of photonic temperature sensors as an alternative to resistance thermometers. These innovative temperature sensors have the potential to leverage advances in frequency metrology to provide cost effective measurement solutions. Here we present the results of our effort in developing novel photonic temperature sensors. Our preliminary results indicate that using photonic devices such as the ring resonators, photonic crystal cavities and Bragg reflectors we can achieve measurement capabilities that are on-par or better than the state of the art in resistance thermometry.

1. Introduction

Resistance thermometry plays a crucial role in various aspects of industry and every-day technology ranging from medicine, manufacturing process control, to environmental process control and oil-and-gas industry [1–3]. Although industrial resistance thermometer can measure temperature with uncertainties as small as 10 mK, they have several unfavorable properties such as hysteresis, sensitivity to humidity and chemical residues, susceptibility to mechanical shock and thermal stress requiring frequent costly recalibration of the sensors [3]. These fundamental limitations have fostered efforts in developing alternative technologies such as photonics to replace legacy devices. A variety of novel photonic thermometers has been proposed recently including photosensitive dyes [4], hydrogels [5], fiber Bragg grating (FBG) [6–8], and on-chip integrated silicon photonic nanostructures [1,9–12].

2. Photonic Thermometry Research at NIST

Given the drawbacks and limitations of legacy-based resistance thermometry we have started photonic thermometry research project at NIST with the aim to develop novel photonic-based sensors and standards that would outperform resistance-based standards. Our goal is to develop a low-cost, readily deployable, novel temperature sensor that can be easily manufactured with the existing technology. In this work we give an overview of three of our on-going thermometry projects: the whispering gallery mode resonator (WGMR), fiber Bragg gratings (FBG) and silicon photonic-based nanosensors. The order in which we describe the thermometry projects

represents the improvement of a photonic-based thermometer, going from the earliest generations (WGMR) to the latest (silicon photonic nanosensors) with improved performance.

3. Whispering Gallery Mode Resonator

For the last 40 years, WGMRs fabricated with a wide variety of materials including polysterene, fused quartz, glass spheres and mono-crystalline synthetic sapphire have been demonstrated as ultra-stable resonators [13,14]. Considerable effort has been expended in eliminating thermal drift of WGMR resonance frequency to improve their frequency stability [15,16]. The temperature dependence of WGMR derives from the thermo-optic effect i.e. the intrinsic temperature dependence of the refractive index (or permittivity) of the material e.g. sapphire.

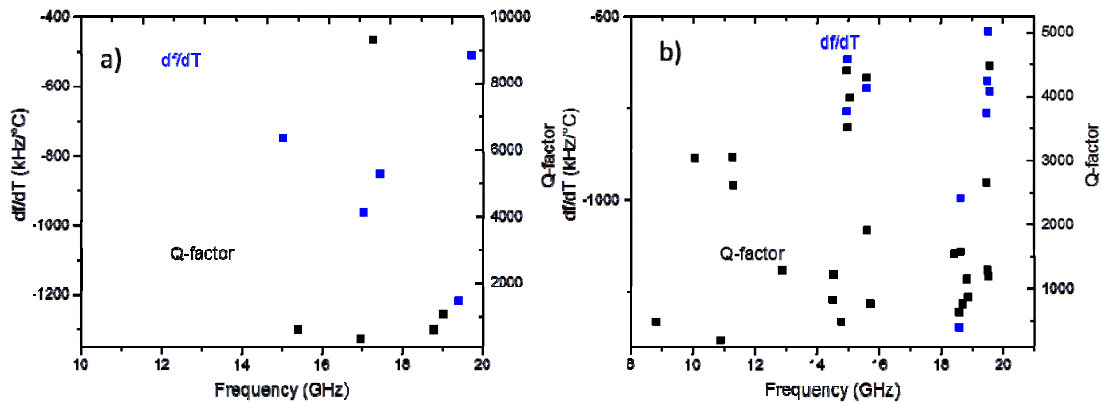


FIG. 1: Q-factor and temperature induced frequency shift of cylindrical (a) and Bragg resonator (b) with Bragg period of 5 mm.

We have exploited the large temperature dependence of sapphire WGM's frequency and the ease of measuring peak frequency of high-Q modes to develop highly sensitive and accurate temperature sensors. Using a disk of monocrystalline sapphire we demonstrated temperature measurement uncertainty ($k = 2$) of 10 mK between 273.15 K and 373 K [14]. Sapphire WGMR thermometers with spherical and cylindrical geometries have also been demonstrated. Recently we examined the impact of mechanical stabilization structures on device performance. Our results indicate the metal support structures, as compared to Teflon support structures, contribute to increased losses of the resonator which results in significant reduction in resonator mode's quality factors (Q-factor) and lower the temperature dependent sensor response by $\approx 40\%$. The reduction of mode Q-factors could potentially be compensated by using Bragg resonators. Our preliminary results (Bragg period of 5 mm with 50% duty cycle) indicate increased mode density and a small increase in overall Q-factors of all resonant modes with minimal impact on temperature dependence (Fig. 1).

4. Fiber Bragg Grating Thermometer

FBGs are narrow band filters commonly used in the telecommunications industry for routing information. FBG are fabricated using photo-sensitive optical fibers (e.g H_2 loaded Ge doped fibers) that are exposed to spatially varying UV light that modifies the local structure of silica, creating a periodic variation in the local refractive index that acts like a Bragg grating [17–19].

Wavelength of light resonant with the Bragg period is reflected back, while non-resonant wavelengths pass through the grating. The grating equation is given by:

$$\lambda_B = 2n_e L$$

where n_e is the effective refractive index and L is the grating period. Change in surrounding temperature impacts the effective grating period due to linear thermal expansion of the optical fiber and its refractive index due to temperature (thermo-optic effect). Existing literature indicates FBG show a temperature dependent shift of ~ 10 pm/K [6,7,18,19] although there is disagreement on whether the FBG temperature response is linear or quadratic. Our preliminary results indicate that over the temperature range of 233 K to 393 K FBG show a quadratic dependence on temperature (Fig. 2) with measurement uncertainty of ≈ 500 mK.

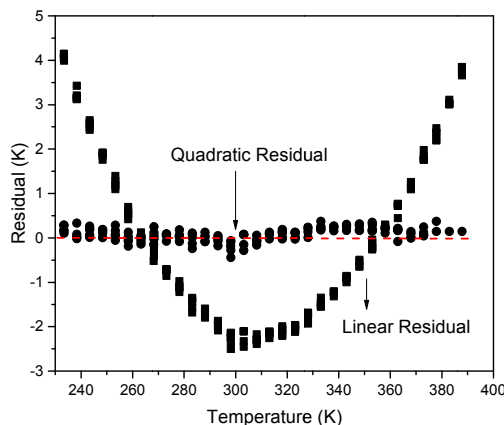


FIG. 2: FBG show a quadratic dependence on temperature over the range of 233 K to 393 K

5. Silicon Photonic Thermometers

Silicon photonic thermometers can be fabricated using silicon-on-insulator (SOI) wafers applying conventional CMOS-technology via photo- or electron beam lithography followed by inductive plasma reactive ion etch (ICP RIE) of 220 nm-thick topmost silicon layer. After ICP RIE etch the devices are top-cladded with thin poly(methyl methacrylate) (PMMA) or SiO_2 protective layer. Below we show and compare the performance of several types of silicon photonic thermometers: nano-waveguide Bragg grating (Si WBG), photonic crystal (Si PhC), ring resonator, nano-waveguide Bragg grating cavity (Si WBG-C) and photonic crystal nano-beam cavity (PhC-C) thermometers.

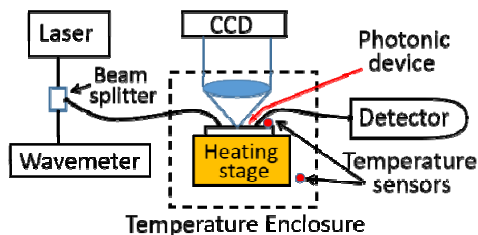


FIG. 3 Schematic diagram of measurement setup for testing photonic-based thermometers

The photonic thermometers are probed using a custom built interrogation system^a (Fig. 3). In this setup a C-band laser (New Focus TLB-6700 series) is swept over the sensor resonance. Ten percent of laser power was immediately picked up from the laser output for wavelength

^a Disclaimer: Certain commercial fabrication facility, equipment, materials or computational software are identified in this paper in order to specify device fabrication, the experimental procedure and data analysis adequately. Such identification is not intended to imply endorsement by the National Institute of Standards and Technology, nor is it intended to imply that the facility, equipment, material or software identified are necessarily the best available.

monitoring (HighFinesse WS/7) while the rest, after passing through the photonic device, was detected by a large sensing-area power meter (Newport, model 1936-R). Light was coupled into and out of the waveguide using grating couplers [20].

5.1. Nano-Waveguide Bragg Grating Thermometer

Figure 4 shows an SEM image of silicon nano-waveguide Bragg grating (Si WBG) thermometer. The device consists of silicon nano-waveguide with a cross section of 510×220 nm which sits on top of $2 \mu\text{m}$ -thick buried oxide (BOX) of SOI substrate. The width of the nano-waveguide is periodically modulated in the square-wave form with 60 nm amplitude and 330 nm pitch. The total length of the sensor is $330 \mu\text{m}$.

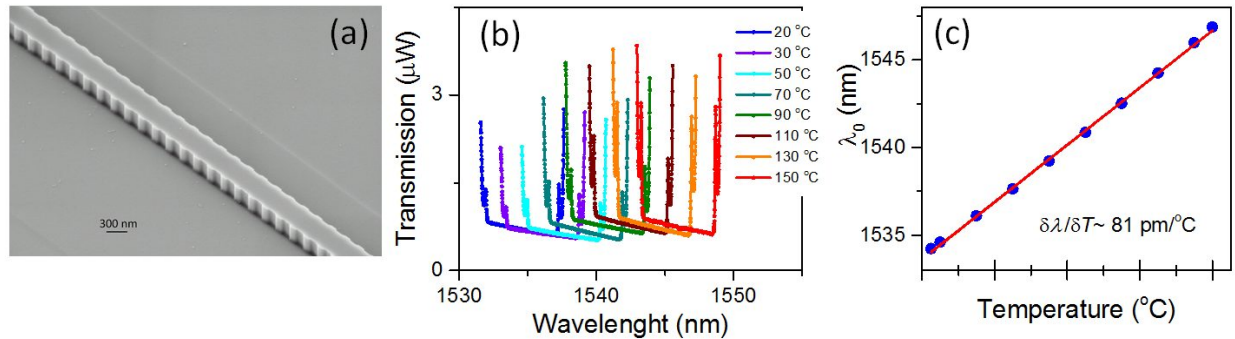


FIG. 4. Nano-waveguide Bragg grating thermometer. (a) SEM image of the part of Si WBG sensor. Waveguide cross section is $220 \text{ nm} \times 510 \text{ nm}$, side wall modulation is 60 nm, pitch – 330 nm. (b) Transmission spectra at different temperatures of SiO_2 -cladded Si WBG thermometer. (c) Temperature dependence of the center of the stop band.

The periodic modulation of refractive index of the nano-waveguide of Si WBG creates a stop band in its transmission spectra. Figure 4(b) shows transmission spectra of SiO_2 -cladded Si WBG thermometer. The stop band width is ≈ 5.2 nm. With increasing temperature the center of the stopband shifts linearly at a rate of $\delta\lambda/\delta T \approx 81 \text{ pm}/^\circ\text{C}$. Our results indicated this Si WBG sensor is capable to measure temperature with resolution of ≈ 0.6 °C.

5.2. Ring Resonator Thermometer

A silicon ring resonator is another type of photonic nanostructure that can be used for temperature sensing applications. It also features microscale footprint and on-chip integration. In recent years, ring resonator [21,22] based devices have been exploited for bio-chemical sensing applications [9,23]. In these sensors, a noticeable temperature dependence of a resonance frequency adversely impacts sensor sensitivity and specificity.

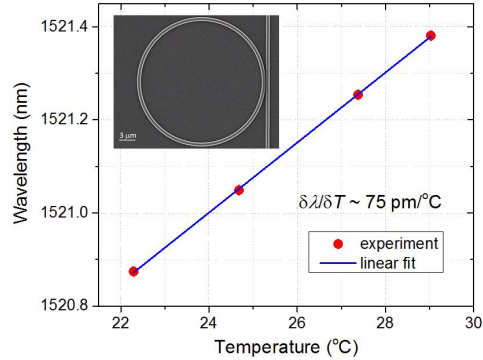


Figure 5. Temperature dependence of ring resonator thermometer cladded with SiO₂. Inset shows SEM image of the device. Ring radius is 11 μm, a gap between the bus waveguide and the ring is 130 nm.

We recently demonstrated that silicon-based optical ring resonator can be used for ultra-sensitive thermal measurements. In particular we showed that a device with a ring diameter or 11 μm and gap (between waveguide and ring) of 130 nm can be a used as a photonic thermometer (Fig. 5) with temperature resolution of 1 mK and noise floor of 80 μK.

5.3. Photonic Crystal Thermometer

Typical photonic crystal (PhC) thermometer is shown on Fig. 6(a). Similar to Si WBG device it consists of silicon waveguide, which features a periodic modulation of its effective refractive index. In PhC thermometer this is done with the help of periodic array of holes. The width of the waveguide (2.5 μm), the diameter of holes (150 nm) and the pitch (276 nm) are chosen such that a photonic band gap has a width ≈ 7.9 nm and is centered around 1540 nm (Fig. 6(b)). The devices shown on Fig. 6(a) was cladded with 800 nm of SiO₂. This band gap shows a temperature-dependent linear shift of $\delta\lambda/\delta T \approx 82$ pm/°C with temperature resolution of ≈ 1.6 °C. Our preliminary results indicates that temperature sensitivity and resolution of PhC device is very comparable to parameters of Si WBG thermometer.

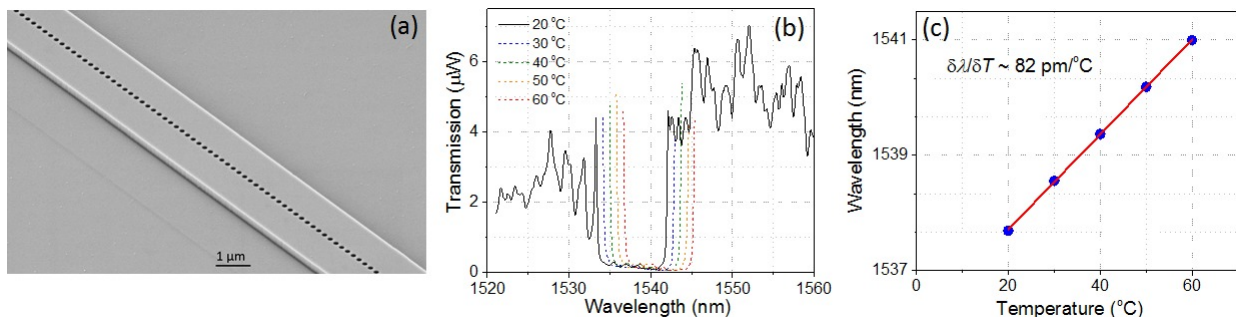


Figure 6. Photonic crystal thermometer. (a) SEM image of the part of PhC sensor. Waveguide cross section is 220 nm × 2.5 μm, hole diameter is 150 nm, pitch – 276 nm. (b) Transmission spectra at different temperatures of SiO₂-cladded PhC thermometer. (c) Temperature dependence of the center of the photonic band gap.

5.4. Nanowaveguide Bragg Grating Cavity Thermometer

Silicon nanowaveguide Bragg grating cavity (Si WBG-C) thermometer is a photonic nanostructure made of SOI nanowaveguide. It features a nanoscale Fabry-Perot (F-P) cavity and two waveguide Bragg mirrors placed on two opposite sides of the F-P cavity. Figure 7 shows the SEM image of the center part of Si WBG-C thermometer. The F-P cavity dimensions are 510 nm (width), 220 nm (thickness) and 327 nm (length). Bragg grating mirrors have the same structure as Si WBG described above – the nanowaveguide's width is periodically modulated in the form of a square wave with modulation amplitude of 60 nm and a pitch of 330 nm. The total length of Si WBG-C including two Bragg mirrors is $\approx 66 \mu\text{m}$.

Figure 7(b) shows transmission spectra PMMA-cladded Si WBG-C thermometer measured at various temperatures between 20 °C and 40 °C. We designed the stop band of the sensor to be $\approx 13.3 \text{ nm}$. At 20 °C the edges of the stop band are located at 1553.6 nm and 1567.0 nm. At the center of stop band there is a resonance peak of quality factor of $Q \approx 3,100$ (FWHM $\approx 500 \text{ pm}$). The temperature dependence of resonance wavelength plotted on Fig. 7(c) shows a linear temperature dependence of $\delta\lambda/\delta T \approx 70 \text{ pm}/^\circ\text{C}$. Given the peak width of $\approx 500 \text{ pm}$, we can reliably resolve temperature differences of 0.7 °C. Temperature resolution can be further improved in the future by fabricating higher Q devices.

5.5. Photonic Crystal Nanobeam Cavity Thermometer

Silicon photonic crystal nanobeam cavity (PhC-C) thermometer is another type of F-P nanostructure. A silicon nanowaveguide of width of 800 nm is pattern with a one dimensional array of nanoholes of diameters ranging from 170 nm to 230 nm. Nanoholes form two Bragg mirrors enclose a F-P cavity. In designing the PhC-C sensors we followed a deterministic approach described in Refs. [24,25]. In this approach the F-P cavity is of zero-length, while the Bragg mirrors have a Gaussian field attenuation, which, in turn, maximize the Q of the cavity.

Figure 7(d) shows the center part of Si PhC-C sensor. The zero-length F-P cavity is located at the very center of the SEM image. Figure 7(e) shows the transmission spectra of PMMA-cladded Si PhC-C device measured at different temperatures and Fig. 7(f) represents a temperature dependence of resonance peak corresponding to the fundamental mode. The sensitivity of PhC-C is $\delta\lambda/\delta T \approx 70 \text{ pm}/^\circ\text{C}$, with temperature resolution of 0.07 °C.

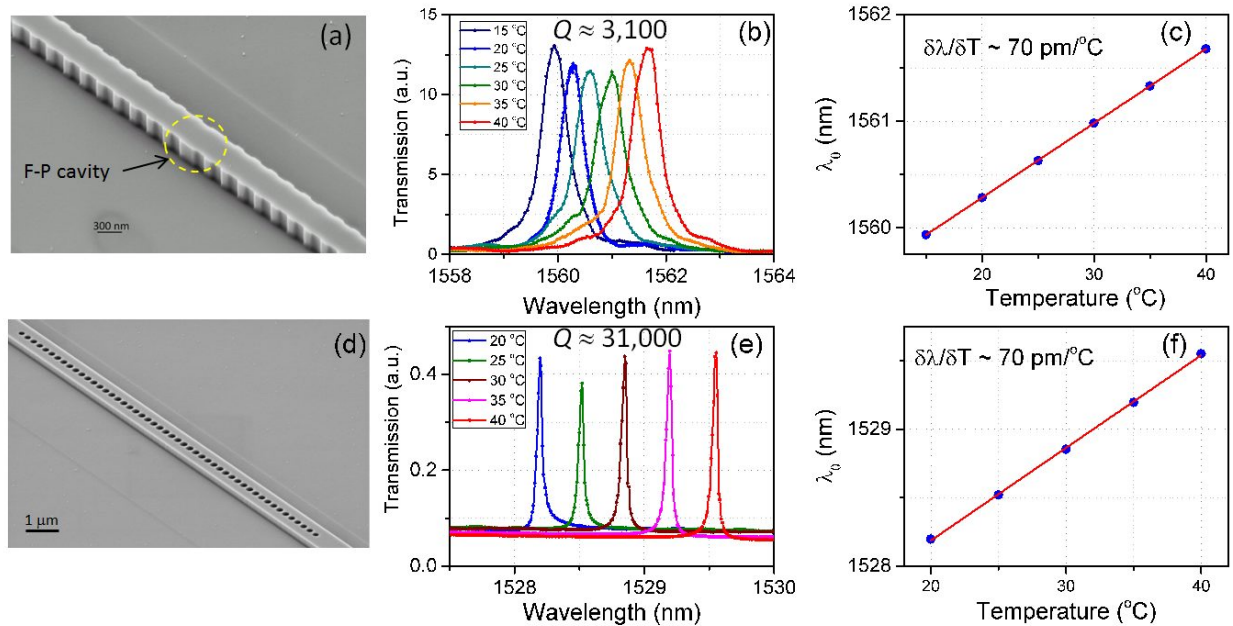


FIG. 7. Fabry-Perot cavity-based silicon photonic thermometers. (a) SEM image of the center cavity part of uncladded Si WBG-C thermometer. F-P cavity is marked by a yellow circle. (b) Transmission spectra of PMMA-cladded Si WBG-C at different temperatures. (c) Temperature dependence of the resonance wavelength of PMMA-cladded Si WBG-C. (d) SEM image of uncladded Si PhC-C thermometer. (e) Transmission spectra of the fundamental mode of PMMA-cladded Si PhC-C. (f) Temperature dependence of the resonance wavelength of PMMA-cladded Si PhC-C.

6. Summary

The fundamental limitations of resistance-based thermometers ignited substantial interest in developing alternative temperature sensors. In the paper we present an overview of ongoing photonic thermometry research at NIST. We cover various types of photonic thermometers from WGMR, operating at microwave frequencies, to FBG and silicon photonic nanosensors, working at telecom frequency range. It has been shown that photonic-based thermometers can provide low-cost temperature measurement capability that is on par, if not better than legacy-based sensors.

Acknowledgement

The authors acknowledge the NIST/CNST NanoFab facility for providing opportunity to fabricate silicon photonic temperature sensors.

References

- [1] H. Xu, M. Hafezi, J. Fan, J. M. Taylor, G. F. Strouse, and Z. Ahmed, *Opt. Express* **22**, 3098 (2014).
- [2] F. A. Jolesz, *Annu. Rev. Med.* **60**, 417 (2009).
- [3] G. F. Strouse, *NIST Spec. Publ.* **250**, 81 (2008).

- [4] J. S. Donner, S. A. Thompson, M. P. Kreuzer, G. Baffou, and R. Quidant, *Nano Lett.* **12**, 2107 (2012).
- [5] E. M. Ahmed, *J. Adv. Res.* **6**, 105 (2015).
- [6] S. J. Mihailov, *Sensors* **12**, 1898 (2012).
- [7] A. Kersey and T. A. Berkoff, *IEEE Photonics Technol. Lett.* **4**, 1183 (1992).
- [8] Y.-J. Rao, D. J. Webb, D. . Jackson, L. Zhang, and I. Bennion, *J. Light. Technol.* **15**, 779 (1997).
- [9] M.-S. Kwon and W. H. Steier, *Opt. Express* **16**, 9372 (2008).
- [10] B. Guha, B. B. C. Kyotoku, and M. Lipson, *Opt. Express* **18**, 3487 (2010).
- [11] B. Guha, K. Preston, and M. Lipson, *Opt. Lett.* **37**, 2253 (2012).
- [12] G.-D. Kim, H.-S. Lee, C.-H. Park, S.-S. Lee, B. T. Lim, H. K. Bae, and W.-G. Lee, *Opt. Express* **18**, 22215 (2010).
- [13] A. A. Savchenkov, A. B. Matsko, V. S. Ilchenko, N. Yu, and L. Maleki, *J. Opt. Soc. Am. B* **24**, 2988 (2007).
- [14] G. F. Strouse, *Int. J. Thermophys.* **28**, 1812 (2007).
- [15] D. L. Creedon, M. E. Tobar, J.-M. Le Floch, Y. Reshitnyk, and T. Duty, *Phys. Rev. B* **82**, 104305 (2010).
- [16] R. Boudot, C. Rocher, N. Bazin, S. Galliou, and V. Giordano, *Rev. Sci. Instrum.* **76**, 095110 (2005).
- [17] S. J. Mihailov, *Sensors* **12**, 1898 (2012).
- [18] J. Hetch, *Understanding Fiber Optics*, 4th. ed. (Princeton Hall, 2002).
- [19] D. A. Krohn, *Fiber Optic Sensors: Fundamentals and Applications*, 3rd ed. (ISA, 2000).
- [20] F. Van Laere, G. Roelkens, M. Ayre, J. Schrauwen, D. Taillaert, D. Van Thourhout, T. F. Krauss, and R. Baets, *J. Light. Technol.* **25**, 151 (2007).
- [21] W. W. Rigrod, *Bell Syst. Tech. J.* **44**, 907 (1965).
- [22] L. Stern, I. Goykhman, B. Desiatov, and U. Levy, *Opt. Lett.* **37**, 1313 (2012).
- [23] X. Tu, J. Song, T.-Y. Liow, M. K. Park, J. Q. Yiyang, J. S. Kee, M. Yu, and G.-Q. Lo, *Opt. Express* **20**, 2640 (2012).
- [24] Q. Quan, P. B. Deotare, and M. Loncar, *Appl. Phys. Lett.* **96**, 203102 (2010).
- [25] Q. Quan and M. Loncar, *Opt. Express* **19**, 18529 (2011).